Multidimensional Analytical Study of Heart Sounds: A Review

Akash Kumar Bhoi[1*], Karma Sonam Sherpa[2], Bidita Khandelwal[3]

[1]*Department of Applied Electronics* and *Instrumentation Engineering*
Sikkim Manipal Institute of Technology
Majhitar, India
E-mail: akash730@gmail.com

[2]*Department of Electrical* and *Electronics Engineering*
Sikkim Manipal Institute of Technology
Majhitar, India
E-mail: karmasherpa23@gmail.com

[3]*Department Gen Medicine*
Central Referral Hospital and SMIMS, SMU
Gangtok, India
E-mail: drbidita@gmail.com

[*]*Corresponding author*

Received: April 15, 2015 **Accepted: September 23, 2015**

Published: September 30, 2015

Abstract: *Heart diagnosis by phonocardiography and auscultation is highly dependent on experience and there is a considerable inter-observer variation. The complex structure of the Phonocardiogram (PCG) and the variations due to cardiac contractility can generate additional difficulties for auscultation. This review paper focuses on such critical problem solving issues with a variant of analysis. However, different methods and techniques are also described for detection and analysis of PCG signal and it will certainly aid findings in novel computational tools in biosignal processing.*

Keywords: *Phonocardiography, Variant Analysis, Multidimensional Analysis.*

Introduction

Heart sounds and murmurs arise as a consequence of turbulent blood flow and vibrating cardiovascular structures. Some decades ago, the Phonocardiography (PCG) has been largely used together with the Electrocardiography as providing important information about the cardiac diseases. Later, the ultrasound techniques took its place offering a lot of additional quantitative indices related to the cardiovascular system. Recently the interest to the PCG and other more sophisticated heart sounds investigations reappears in the field of medicine [88]. The reason is that they are non-invasive, economical and accurate methods for assessing different heart valve pathologies. Hult et al. [88] suggested that the detection of a third sound in adults is shown as simple method for systolic heart failure discovery.

The PCG signal discloses information about cardiac function through vibrations caused by the working heart. In the early days of PCG signal analysis, manual interpretation of waveform patterns was performed in the time domain. Heart sounds were identified as composite oscillations related to valve closure and heart murmurs seemed to derive from malfunctioning valves or from abnormal holes in the septal wall [1]. Heart auscultation, the technique of listening to heart sounds, is a convenient and economical method for diagnosing cardiovascular diseases (CVD). Though clinical diagnosis of cardiovascular disease mainly

refers to other methods such as electrocardiography (ECG), angiocardiography and so on, the considerable role of PCG in diagnosis of CVD cannot be underestimated, especially in computer-aided CVD diagnosis of fusing other vital signals (e.g. ECG) to improve the diagnostic accuracy [66]. The physiological variability of the mechanical function of the heart is reflected in the produced acoustic vibrations – the heart sounds. Heart sounds have been widely used in clinical practice since the introduction of the first stethoscope by Laennec in 1816, and the invention of phonocardiography, the graphic recording of heart sounds, by Einthoven in 1894. Heart sounds and their clinical utilization in cardiovascular and cardiopulmonary diseases have been extensively studied for many years [36]. Relations between morphological features of heart sounds and hemodynamic parameters have been quantitatively described in both animal models and humans [37, 38].

Heart sounds and murmurs are of relatively low intensity and are band-limited to about 10-1000 Hz, (Fig. 1).

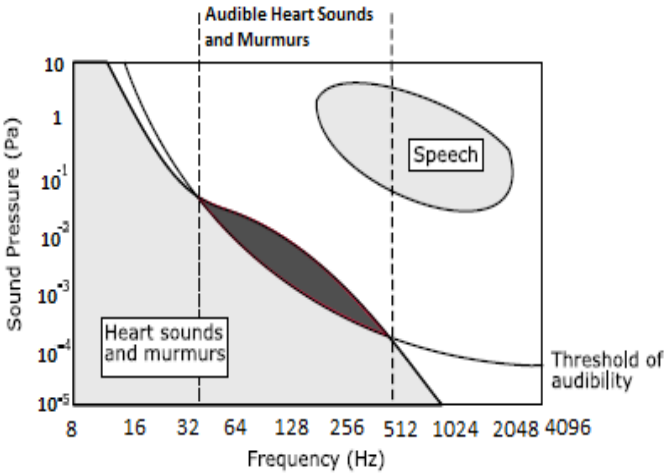

Fig. 1 Relationship between the acoustic range of cardiac sounds and the threshold of audibility of sound pressure for human ear
(figure redrawn from Leatham [2])

The traditional areas of auscultation (Fig. 2), where the radiated sound intensity from each of the four heart valves is maximized, are defined as [5]:

- Mitral area: The cardiac apex.
- Tricuspid area: The fourth and fifth intercostal space along the left sterna border.
- Aortic area: The second intercostal space along the right sternal border.
- Pulmonic area: The second intercostal space along the left sternal border.

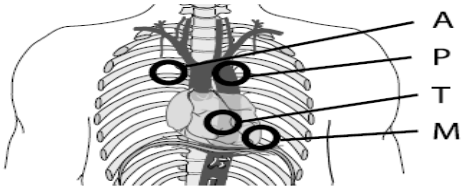

Fig. 2 The traditional auscultatory areas on the chest:
M (refers to the mitral area), T (refers to the tricuspid area),
P (refers to the pulmonic area), and A (refers to the aortic area).

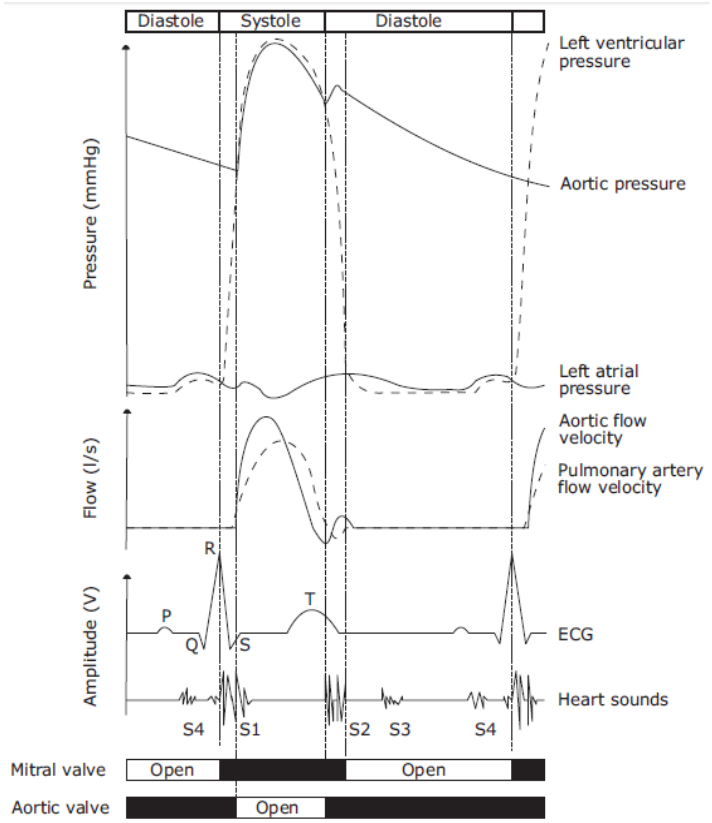

Fig. 3 Wiggers diagram, showing pressures and flows in the left side of the heart over one heart cycle and their relation to electrical (ECG) and mechanical (PCG) activity

The first heart sound (S1) and second heart sound (S2) in Wiggers diagram (Fig. 3) are easily audible in nature, and the time duration is around 150 ms and 120 ms. It ranges from 20 to 150 Hz. Heart sound (S1) is associated with the closure of the mitral-tricuspid valve, it occurs during the isovolumetric contraction of the ventricles. Heart sound (S2) is related to the aorticpulmonary valve at the time of the isovolumetric relaxation of the ventricles. The third heart sound (S3) and fourth heart sound (S4) are very light sound, i.e., almost inaudible in nature. S3 and S4 are very low frequency sound. S3 is not originated from the valve although it happens at the beginning of the diastole and hence, it is known as Proto-diastolic sound. Bulk of blood flow into the left ventricles causes vibrations in the valve. Heart sound (S4) is mainly found in the healthy children and not, usually found in adults. It is called pre-systolic gallop in pathological term when found in adult. The Healthy signals are the signals which have a clear sound of S1 (‘lup’) and S2 (‘dup’) and almost negligible sound of S3 and S4. Healthy heart sound contains heart sound segment S1 and S2, which gives information of functionality of heart sound [3, 4]. The intensity of the first heart sound (S1) varies with certain conditions. Those who suffer from emphysema, obesity, pericardial effusion, myocardial disease or mitral regurgitation may have decreased first heart sound (S1). Increase in intensity of the first sound depends upon the vigour of the ventricular systole. Thus results in loud sounds in exercise, emotional states and in hyperthyroidism, anemia, mitral stenosis and hypertension. The conditions giving rise to change in intensity of the first heart sound (S1) has been discussed by various authors [89-92].

The relationship between ECG and PCG can be figured out from Wingger diagram (Fig. 3) where, S1 occurs with low frequency vibrations approximately 0.05 second after the onset of QRS-complex of ECG signal. S2 starts approximately 0.03-0.05 second after the end on T wave of the ECG. S3 starts at 0.12-0.18 second after the onset of second heart sound (S2)

and the fourth heart sound (S4) starts approximately 0.12-0.18 s after the onset of P wave of ECG signal. S1 and S2 have two major components, M1 and T1, A2 and P2, respectively. M1 is caused by mitral closure and blood flowing interruption in left atrial and systolic ventricular and T1 is caused by tricuspid closure. A2 starts before aortic valve closed, and P2 starts after pulmonary value closure, both are caused by intraventricular pressure dropping and blood returning in diastole. The delay time between M1 and T1, A2 and P2 are called the first split and the second split, respectively. The measurement of the first and second split, lower or higher than 30 ms, will easily make it possible to make discrimination between the normal or pathological type [68]. It is often followed by echocardiography during the abnormal auscultatory findings. However, the lack of reliability of ordinary auscultation its expense and awkwardness of echocardiography make it desirable to develop a more practical, inexpensive, reliable and non-invasive approach to auscultation, one that could also be adapted for continuous monitoring [71-75]. Akbari et al. [76] performed Digital Subtraction Analysis of the heart murmurs signal using a custom computer program called Murmurgram for the detection and characterization. In essence, this program subtracts the recorded sound from two adjacent cardiac cycles to produce a difference signal, herein called a "murmurgram" [76].

Feature extraction is typically a preceding step for a classification or regression task. Heart sound classification, based on morphological spectral and time–frequency features, has been previously used for assessing the condition of bioprosthetic heart valves [40-42]. Auscultation, the noninvasive cardiac testing, is used as a primary detection tool for diagnosis of heart valve disorders since invention of stethoscope in 1816 by Lannec [47]. In Bender, it is reported that few heart valve diseases are best detected only by means of auscultation process [48]. Auscultation is the most common and cost-effective technique, continues to provide an important source of clinical information related to heart valves and also, cannot be totally replaced by alternative technical methods like echocardiography [49]. In case of abnormal heart sounds, there could be several other sounds in the PCG signal besides primary heart sounds. Murmurs are abnormal heart sounds and refer to different pathological conditions as per location, shape, duration and other associated features [52]. Murmurs are generally high-frequency, noise like sounds that are produced as a result of turbulent blood flow. Different features of PCG signals like intensity, frequency content, split information, time relations etc. are helpful in detecting heart valve diseases, if any and the state of the heart function [53]. Ian Cather has presented Artificial Neural Network (ANN) as a discriminative model for classification of five different heart sounds taken from 48 recordings of nine different subjects using wavelet based feature extraction technique [54]. Ölmez et al. [55] have given a classification technique that utilizes Daubechies-2 wavelet detail coefficients at the second decomposition level for classification of seven different heart sounds collected from 28 subjects using ANN. Reed et al. [56] have described a computer-aided diagnosis mechanism for five different pathological cases using seven level wavelet decomposition, based on a Coifman fourth order wavelet kernel and Ari et al. [57] proposed, a binary decision on heart sound, whether pathological or not, in a Digital Signal Processor based system. Choi [58] proposed a technique for detection of valvular heart sounds as normal or pathological using wavelet packet decomposition and support vector machine with fifth order polynomial kernel function. Information, such as the temporal localization of the heart sounds, the number of their internal components, their frequency content, and the significance of diastolic and systolic murmurs, could all be studied directly on the PCG signal. In order to recognize and classify cardiovascular pathologies, advanced methods and techniques of signal processing and artificial intelligence need to be used. The advancement of technology has paved the way for signal processing methods to be implemented and applied in many simple

tools useful in everyday life. This is most notable in the medical technology field where contributions involving the intelligent applications have boosted the quality of diagnosis. Proposing an objective signal processing method capable to extract relevant information from biosignals is a great challenge in telemedicine and auto-diagnosis fields [86]. Sa-Ngasoongsong et al. [87] presented the design and testing of a wireless sensor system developed using a Microchip PICDEM developer kit to acquire and monitor human heart sounds for phonocardiography applications. This system can serve as a cost-effective option to the recent developments in wireless phonocardiography sensors that have primarily focused on Bluetooth technology. This wireless sensor system has been designed and developed in-house using off-the-shelf components and open source software for remote and mobile applications. The small form factor (3.75 cm × 5 cm × 1 cm), high throughput (6,000 Hz data streaming rate) and low cost ($13 per unit for a 1,000 unit batch) of this wireless sensor system make it particularly attractive for phonocardiography and other sensing applications. The experimental results of sensor signal analysis using several signal characterization techniques suggest that this wireless sensor system can capture both fundamental heart sounds (S1 and S2) and is, also, capable of capturing abnormal heart sounds (S3 and S4) and heart murmurs without aliasing. The results of a denoising application using Wavelet Transform show that the undesirable noises of sensor signals in the surrounding environment can be reduced dramatically. The exercising experiment results also show that this proposed wireless PCG system can capture heart sounds over different heart conditions simulated by varying heart rates of six subjects over a range of 60-180 Hz through exercise testing [87]. Shub [50] compared the cardiac physical examination with echocardiography for evaluating systolic murmurs and concluded that echocardiography is not required for all patients with systolic murmurs and should not replace cardiac physical examination; Chizner [51] reviewed the fundamental principles of the art of cardiac auscultation and emphasized on the proper use of the stethoscope and the diagnostic and prognostic significance of the myriad heart sounds and murmurs present in patients with and without symptomatic heart disease, and Debbal et al. [67] proposed computerized analysis of heart sounds which is concerned with a synthesis study of the Fast Fourier Transform (FFT), the Short-time Fourier Transform (STFT), the Wigner distribution (WD) and the Wavelet Transform (WT) in analyzing the Phonocardiogram signal (PCG). It is shown that these transforms provide enough features of the PCG signals that will help clinicians to obtain qualitative and quantitative measurements of the Time-frequency (TF) PCG signal characteristics and consequently aid diagnosis.

Physiological importance of heart sounds

Fetal maturity

As during pregnancy all the frequency determining parameters undergo physiological change. The growing dimensions and increasing contractile strength of the myocardium characteristic changes of the PCG spectrum are to be expected as a function of the stage of fetal maturity. In order to verify this assumption, extensive experimental studies have been done. The power spectra were integrated in order to compare different spectra using only one single parameter. The determining measure was the frequency within which 80% of the total PCG power is contained, i.e., where the power spectrum integral reaches 80% of its maximum. Mean values of the 80% marks for the first and second heart sound are shown in Fig. 4. Each point was computed from 30-50 fetuses of the same gestational age. Of course, mean values have been computed only from spectra of fetuses that were known to be developing normally.

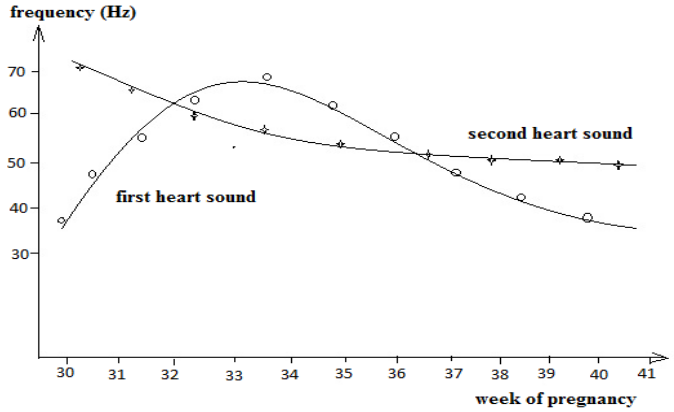

Fig. 4 Relationship between fetal PCG spectrum and gestational age.
The traces show the mean 80% power marks of the integrated power spectra
for the first and second heart sound dependent on the week of pregnancy.
The standard deviation of the single measuring points typically corresponds to 1.4 weeks.
(figure redrawn from Nagel [16])

The first heart sound reveals a steady shift towards higher frequencies up to about the 34th week of gestation. Thereafter, the shift reverses its direction. The spectrum of the second heart sound steadily shifts to lower frequencies. The decrease in frequencies can be explained by the growth of the heart from physical models, whereas the ascending slope of the first heart sound's spectrum is primarily caused by the predominance of the increasing contractile strength of the myocardium during that stage of pregnancy. On the basis of these findings, spectral analysis of the PCG can be considered a real alternative to better known measurements such as ultrasonic imaging in the determination of fetal maturity. When investigating the reliability of this measurement, possible disturbing influences such as changing cardiovascular conditions (e.g. the heart rate) have to be considered. So far, however, no negative effects have been found. Indeed, measurements were always done at the basal heart rate with no labor activity, and in the absence of accelerations and decelerations. In several cases the spectra did not fit any stage of maturity, showing distinct deviations from normal values. Further investigations (done partially after birth), confirmed the existence of heart diseases, predominantly valve malfunctions. This diagnostic capability is the direct consequence of the fact that each pathological variation of either cardiac function or anatomy results in a change in the PCG spectrum.

Cardiac contractility variability

Variation in the amplitude of the first heart sound is seen in almost every sample of the Phonocardiogram (PCG). During heart-sound signal processing, Xiao et al. [29] found that this phenomenon had its own regularity. There are many factors causing this variation, such as respiration, exercise, psychological activity, drugs, temperature, smoking, disease, etc. These factors can affect the heart's state of inotropism, chronotropism, and dromotropism, which will be reflected in the PCG. It has been reported that changes in the amplitude of the first heart sound are closely correlated with the maximum rate of rise of left ventricular pressure (a standard measure of cardiac contractility) [23-28].

Descriptive analysis have already being done based on the relationship between the amplitude of the first heart sound (S1) and the cardiac contractility [23-28], Xiao et al. [29] proposed a concept of Cardiac Contractility Variability (CCV) and a method of analysis. This study was carried out to examine the regularity of the amplitude variability of the first heart sound and to evaluate the practical significance of the CCV. Cardiac contractility variability can easily be

studied by means of heart-sound analysis, a safe, non-invasive, and inexpensive technique. Analyzing the regularity of S1 variability and evaluating CCV may have practical utility and is worth further study. A study of CCV may be of help in gaining insight into the neurogenic cardiovascular state of patients in different clinical conditions.
A change in the pattern of CCV may be an indicator of systolic function. Also, it might be an indicator of lung ventilation function e.g., in a patient with emphysema, the compliance of lungs and thorax decreases. In turn, the respiratory variation of venous return to the heart is reduced, and therefore the variation of S1 amplitude in a respiratory cycle becomes less obvious.

Spectral analysis of prosthetic heart valve sounds

Analog techniques for processing prosthetic valve Phonocardiograms (PCG) have met with limited success in extracting this information, because of their poor spectral resolution and lack of versatility. Numerical methods of signal processing overcome most of these limitations, but the need for a computer to implement numerical methods raises the question of cost-effectiveness in many applications. Numerical analysis of prosthetic valve signals has, therefore, received very little attention outside the academic and laboratory context. Cost reductions in computer hardware arising from the use of micro-processors; make it possible to envisage dedicated clinical instruments for processing prosthetic valve sounds in view of assessing overall valve performance and detecting component degradation at an early stage. Basic spectral considerations for the design of such instruments are discussed [15].

From the very beginning of phonocardiography, it has been known that sound-producing events which give rise to the PCG include oscillations of blood masses, movements of the heart wall and valves and turbulence in blood flow. Signals recorded from the body surface are further conditioned by the transmission characteristics of intervening tissues and the transducer used. Because these structure (both the active sound producing sources and passive components) differ morphologically. Their vibrational modes of resonance are also different. Fortunately, most prosthetic valve sounds are much louder and contain higher frequency components than the other structures of the heart so that extracting them from the PCG is relatively easy.

In the past, two techniques of spectral analysis (spectroanalysis) have been used for detecting such changes. One technique, called “octave-band analysis” uses a bank of band-pass filters and an electronic system that evaluates the relative energy of the signal output by each filter [6]. The term “octave-band analysis” arises from the fact that the central frequencies of two successive filters are in a ratio of 1:2. An average curve is then obtained by plotting the relative amplitude of prosthetic sounds versus frequency over many cardiac cycles. The other technique named “sound spectrography” was developped by Bell Laboratories for speech analysis; it was first used in phonocardiography by Geckeler et al. [7] and McKusic et al. [8] in 1954. Instruments based on this technique provide a three dimensional display of frequency, amplitude and time for a short segment of PCG recorded on a loop of magnetic tape to reproduce the PCG with the periodicity required for the analysis. The principle of analysis is to use a single fixed band-pass filter and to translate the spectrum of the signal in successive steps. This is achieved through amplitude modulation of the PCG by a sine wave whose frequency is increased step-wise. The spectrum of the PCG is thus progressively swept; the amplitude of each frequency band is evaluated and recorded on photographic paper as dots of variable intensity. A drawback of this instrument was that only a qualitative evaluation of spectral energy was possible from the gray-scale graph. This was overcome by a later instrument introduced by Winer (1965) which presents the signal information as

frequency-time contours of equal spectral energy. It is this later technique that has been mostly used in the non-invasive evaluation of prosthetic ball-valve variance, as reported by Hylen et al. [9] (1969), Aigner et al. [10, 11] (1973-1977), and Kagawa et al. [12] (1977). An example of the spectrum of an aortic valve sound obtained by this technique is presented in Fig. 5.

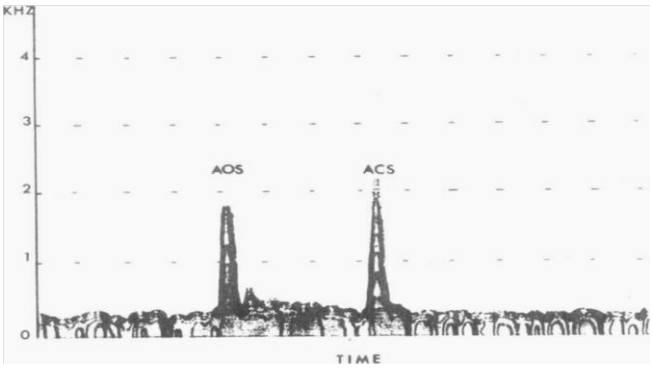

Fig. 5 Contour spectrogram of the PCG of a Harken aortic ball valve:
Aortic opening sounds (AOS), Aortic closing sound (ACS).
(figure redrawn from Durand et al. [15])

Despite the fact that such a representation contains a lot of information on the prosthetic valve being evaluated; the extraction of quantitative parameters is quite difficult. The spectral analysis of prosthetic valve sounds done by octave-band analysis and contour spectrography is mostly qualitative and generates quantitatively the same parameter: the highest harmonic component of opening (OS) or closing valve sounds (CS). Therefore, the information contained in the Phonocardiogram of cardiac valve prostheses. In addition, being essentially analog techniques and the difficulty of implementing filters with near ideal band-pass frequency response, it suffers from limited frequency resolution. While these techniques were finding some limited clinical acceptance whereas, the increasing availability of digital computers in the early '60s promoted the development of numerical methods of signal analysis. One of the most important events of this decade was the introduction of the FFT algorithm by Cooley and Tukey [13] in 1965, which, by drastically reducing the computing time required for spectral evaluation, practically revolutionized signal analysis.

An efficient FFT implementation of the Discrete Fourier Transform (DFT) is crucially important since the DFT is the basis for most spectrum analysis techniques: a speed improvement of roughly 100 in the computation of a 1024 sample sequence can result from the evaluation of the FFT versus the evaluation of spectral components by a straightforward numerical integration. The Discrete Fourier Transform pair can be represented by:

$$X(k) = \sum_{n=0}^{N-1} x(n) W_N^{nk} \ , \ k = 0, 1, \ldots, N-1 \tag{1}$$

$$X(n) = \frac{1}{N} \sum_{n=0}^{N-1} x(k) W_N^{-nk}, \ k = 0, 1, \ldots, N-1 \tag{2}$$

where the amplitude and phase information of the harmonic term $W_n = e^{-j2\pi/N}$ is contained in the complex coefficient $X(k)$.

In order to retain some temporal information of the PCG signal, the concept of the short-time Fourier representation of a signal is quite useful [14]. Mathematically, it can be defined as:

$$X(n,k)=\sum_{m=0}^{N-1}\left(W(m)x\left(n+m-\frac{N}{2}\right)\right)e^{-\frac{j2\pi mk}{N}}, \quad \text{for } k=0,1,\ldots,N-1 \text{ and } -\infty<n<\infty \tag{3}$$

where $W(m)$ is a real window sequence of duration N centered on the time index n in order to determine the portion of the input signal that receives emphasis at a particular value of n. The procedure is illustrated in Fig. 6.

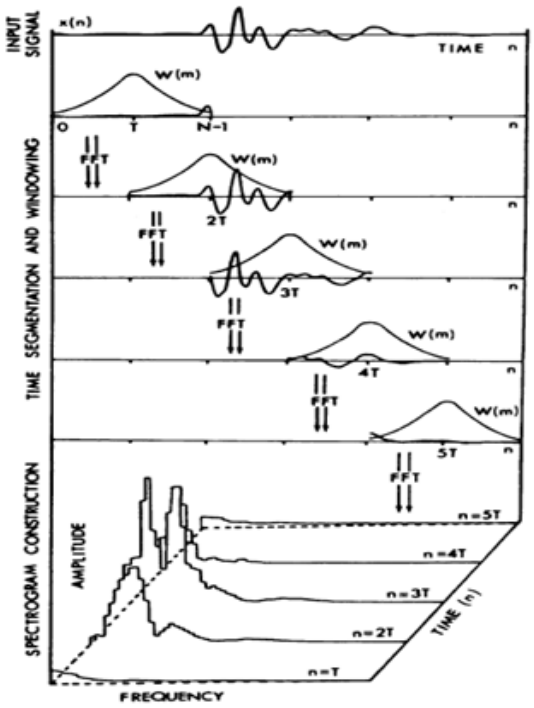

Fig. 6 Schematic illustration of the spectrogram construction of a signal $x(n)$ (figure redrawn from Durand et al. [15])

The short-time DFT is clearly a function of two variables: for each value of the time index n, the obtained Fourier representation (index k) of its neighboring values emphasized by the window sequence used. Thus, by taking successive short-time DFT at each or multiple values of time index n, it is possible to construct a digital time-dependent frequency representation of the input signal.

PCG spectral composition

The heart represents a rather complex oscillatory system, whose spectral power distribution is determined by numerous factors, such as the dimensions of the vibrating tissues (muscle and valves), their properties with respect to elasticity and density, and the physical conditions of vibrational excitation, especially the spectrum of the excitational function and the tension of the tissues that is caused by external forces as well as by their own contraction. Additionally, the spectrum is influenced by the surrounding media, primarily the blood contained in heart and vessels. Last but not least, the intracardial blood volume itself represents a vibrational system, whose contribution to the heart sounds appears particularly distinct in the case of eddy flows caused by cardiac malfunctions, such as valvular stenosis or insufficiency. Due to the complexity of the heart it is not possible to formulate an analytical description of the

vibrations or their spectra. The well-known Laplace model describes the ventricles as a thin-walled hollow sphere. The tension (s) of the wall depends on the trans-mural filling pressure (p), the radius (r) of the sphere, and the thickness (h) of the wall, that is the myocardium:

$$s = \frac{pr}{2h} \tag{4}$$

For thick-walled structures, the relationship is

$$s(r) = \frac{p_i r_i^3 \left(1 + \frac{r_a^3}{2r^3}\right)}{(r_a^3 - r_i^3)} \tag{5}$$

where r_i and r_a represent inner and outer radii of the wall, and r lies between these limits. The tension decreases from the inside towards the outside. In the course of the heart cycle, both wall tension and intracardial pressure and also the radius of the ventricles are subject to change. According to the stage of heart action, these three variables exchange the function of dependent and independent parameters. During diastole there is a passive increase of wall tension (the preload) caused by the filling pressure, whereas during the systole the contraction of the myocardium actively increases the wall tension (the after load) and thus produces an interventricular rise of pressure. During the ejection time, the tension of the myocardial wall is influenced essentially by the decrease in ventricular radius and the increase in its thickness. Besides pathologic variations of the PCG power spectrum, characteristic shifts are also to be expected according to physiological changes of the characteristic parameters that occur depending on gestational age and fetal maturity [16].

Representation of heart sound signal in time-frequency domains

Several signal models can be found in literature for the decomposition of heart sound signal, such as the chirp models [60, 61], the damped sinusoidal models [62, 63], the modified Prony models [64], and Leung et al. [65] employed the Gaussian modulation model to decompose the second heart sound for the diagnosis of pediatric heart diseases. For each patient, the splits of 20 successive cardiac cycles are measured; their mean and standard deviation are then calculated and used to characterize the two splitting patterns. It is found that the two simple statistical quantities can be used to identify the splitting patterns and hence, offer important diagnostic information.

$$h_m(t) = \sum_{i=1}^{L_m} a_{mi} e^{-(t-t_{mi})^2/\left(2\sigma_{mi}^2\right)} \cos(2\pi\omega_{mi} t + \beta_{mi}) \tag{6}$$

where $h_m(t)$ is the heart sound signal of the m^{th} cycle. Namely, Eq. (6) means that $h_m(t)$ is the sum of L_m atoms. Every atom is characterized by five parameters: t_{mi} is the time delay of the i^{th} atom with respect to the start of the m^{th} cycle; a_{mi} is the amplitude; ω_{mi} is the frequency; σ_{mi} is the time width that the atom needs support; β_{mi} is the phase. Therefore, the heart sound signal of this cycle is represented by the set of atoms $\{t_{mi}, a_{mi}, \omega_{mi}, \sigma_{mi}, \beta_{mi}, 1 \le i \le L_m\}$. The number of atoms, L_m, and the five parameters for each atom can be obtained using short-time Fourier transform (STFT) analysis, as described in [65].

The STFT of the heart sound signal $h_m(t)$ is

$$H(t, f) = \int h_m(t)\omega(t-\tau)e^{-2\pi\omega\tau}d\tau \quad (7)$$

Biometric identification

The performance of traditional biometric identification systems is, as yet, unsatisfactory in certain applications. For this reason, other physiological or behavioral characteristics have recently been considered, using new electrical or physical signals linked to a person's vital signs. Francesco Beritelli examines the biometric characteristics of PCG signals from cardiac auscultation. The idea is that PCG signals have specific individual characteristics that can be taken into consideration as a physiological sign used in a biometric system [31]. The database used for the biometric identification by Francesco Beritelli, contains heart sounds from people suffering from various types of cardiac pathology. In order to study the spectral characteristics of heart sounds and, therefore, their biometric properties, the recordings which are used contains heart sounds relating to the following pathologies:

1) innocent systolic murmur; 2) mitral regurgitation variations; 3) mitral regurgitation; 4) mitral stenosis; and 5) third heart sound.

Biometric technologies are based on the use of individual characteristics for the recognition or identification of an individual [30]. They are divided into two areas:

1) Physiological characteristics (unique and unvarying), which include the geometry of the hand and the palm print, fingerprints, retina, or iris image, and the (geometrical) features of the face;

2) Behavioral characteristics (unique but varying), which include signature, way of walking, voice (the latter also belongs to the previous group), and keyboard typing style. A feature common to all biometric technologies is the capability of human recognition from biometric data. This consists of a series of basic processes:

i. Acquisition and storage of reference biometric data acquired by means of sensors (optical, ultrasonic, thermal, etc.);
ii. Acquisition of new biometric data at the start of a recognition process, for comparison with the reference data;
iii. Determination of the correspondence of the newly acquired data to the stored reference to determine whether they both could have been generated by the same person.

In the first phase (enrollment), a sample is acquired, which might be converted to a template, a model, or left unprocessed. This is accomplished in a controlled environment so as to guarantee the security of the original and the properties of the biometric print. The second phase (matching) is activated whenever it is necessary to verify or identify a print. Authentication or verification is performed by comparing the acquired print with a reference. Identification is performed by searching in an archive for a compatible template. They therefore serve to identify a person whose identity is not necessarily known a priori. The implementation of a biometric solution requires recognition threshold values to be assigned. Due to various physical and environmental factors, in fact, the result of a biometric identification process is never completely certain. The definition of the recognition threshold establishes the boundary between acceptance and rejection of a request. In this way, it is possible to set the security level on which the False Reject Rate (FRR) depends on (i.e., the number of times the system does not recognize a sample as coming from the same individual who produced the reference) and the False Accept Rate (FAR) (i.e., the number of times the

system incorrectly matches a sample from one person to a reference from another). The FRR and FAR are generally considered as indices of the biometric system's performance.

The segmentation algorithm, which is essential for the subsequent matching phase, generally segments the sequences analyzed correctly and so is very robust to the degradation typically occurring in PCG sequences recorded in a real application context. As far as the matching phase is concerned, first conducted a preliminary study to identify the heart auscultation region (i.e., one of the four auscultation positions for the stethoscope), which gives the best degree of separability between classes for intra and interperson distances.

Matching algorithm

The metric used to measure the distance between the two signal spectra was Euclidean. Considering the spectra as *N*-dimensional vectors

$$d(X,Y) = \frac{1}{N}\sqrt{\sum_{i=1}^{N}(X_i - Y_i)^2} \tag{8}$$

where *X* and *Y* are the vectors containing samples of the signal spectrum whose distance is to be measured, and is the number of samples calculated for each frame. When S1 and S2 signals are extracted from a cardiac sound recorded from the same individual, the distances with respect to the spectra are expected to yield lower values than those obtained when S1 and S2 spectra extracted from sounds recorded from different individuals are used. Following a series of recordings, the distributions of the distance variable with S1 recordings made from both the same person and different individuals is determined.

Quantitative methods for PCG signal analysis

Matching pursuit method

Zhang et al. [18] developed a time-frequency scaling transformation based on the Matching Pursuit (MP) method for the Phonocardiogram (PCG). The MP method decomposes a signal into a series of time-frequency atoms by using an iterative process [18].

A. Time-scaling of PCG signals

The MP method represents a signal as a combination of an infinite number of time-frequency atoms [17]. It can be written as

$$x(t) = \sum_{i=0}^{+\infty} a_i h_i(t) \tag{9}$$

with

$$h_i(t) = \beta_i g_i(t) u_i(t) \tag{10}$$

and

$$g_i(t) = g\left(\frac{t - p_i}{s_i}\right)$$
$$u_i(t) = \cos(2\pi f_i t + \phi) \tag{11}$$

where a_i are the expansion coefficients. The parameters (s_i) (the scale factors) are used to control the width of the waveform envelope, and (p_i) are used to specify their temporal location. The parameters β_i are normalizing factors to keep the norm of $h_i(t)$ equal to one.

The purpose of time scaling the PCG is to change the rate of presentation while keeping the perceptual quality of the original signal. For a uniform change in the time scale, the time t of the original PCG is mapped into the transformed time scale t' through the mapping

$$t' = \gamma t \tag{12}$$

Zhang et al. [18] found that the time scale expansion is more useful than time scale compression. Thus, γ is always larger than one. In the MP method, the temporal properties of a time-frequency atom are related with the time-position (p_i) and the scale (s_i) which are modified for time-scaling of the PCG. For an input signal $x(t)$, the reconstructed signal $x'(t)$ by the MP method for m time-frequency atoms is given by

$$x'(t) = \sum_{i=0}^{m-1} a_i g_i \left(\frac{t - p_i}{s_i} \right) \cos(2\pi f_i t + \phi) \tag{13}$$

For time scaling, the time-position and scale factors are modified to give

$$p_i' = \gamma p_i \,,\; s_i' = \gamma s_i \tag{14}$$

The module, frequency and phase are not changed, so that the time-scaled version is

$$x'(t') = \sum_{i=0}^{m-1} a_i g_i \left(\frac{t' - \gamma p_i}{\gamma s_i} \right) \cos\left(2\pi f_i t' + \phi_i\right) \tag{15}$$

B. Frequency-scaling of PCG signals

Frequency-scaling by the MP method is performed by scaling the frequency *(f)* of each time-frequency atom of the signal by using

$$f' = \xi f \tag{16}$$

where ξ is a scaling constant.

Thus, the frequency-scaled signal can be expressed as

$$x'(t) = \sum_{i=0}^{m-1} a_i g_i \left(\frac{t - p_i}{s_i} \right) \cos\left(2\pi\xi f_i t + \phi_i\right) \tag{17}$$

C. Joint time-frequency scaling of PCG signals

Sometimes a joint time-frequency scaling is desired for changing both the time and the frequency properties of a signal. The transformation is the combination of the time scaling and the frequency-scaling described above. Thus,

$$x'(t') = \sum_{i=0}^{m-1} a_i g_i \left(\frac{t' - \gamma p_i}{\gamma s_i} \right) \cos\left(2\pi\xi f_i t' + \phi_i\right) \quad (18)$$

Array phonocardiography

The feasibility of applying passive listening array technology to the detection and localization of audible acoustic signals in the human body is discussed. A primary clinical objective is the low cost, non-invasive early diagnosis of Coronary Artery Disease (CAD). Referred to as array Phonocardiography, the technique uses an array of vibration sensors placed non-invasively on the external chest wall. A wave speed dispersion curve permits focusing of a scanning beam to an array near field focal point that is scanned over a desired volume to form an intensity image. A model for blood flow induced vibrations of a diseased coronary artery is used to compare with experimental, in vitro, results using a urethane phantom. A turbulence source can be located within 1 cm imaging using both a time delay-and-sum Conventional Beam Former (CBF) and a reduced rank Adaptive Beam Former (rrABF). The performance of the rrABF is sensitive to the spatial extent of the radiating near field source; however, the imposition of a spatial gain constraint mitigates the problem [19]. Irregularities using near field focused beam forming techniques has been suggested as a procedure that would enhance listening performance and serve as a non-invasive, diagnostic screening device [20-22].

Neural network classification

A novel method for segmentation of Heart Sounds (HSs) into single cardiac cycle (S1-Systole-S2-Diastole) using homomorphic filtering and K-means clustering is presented by Gupta et al. [32]. Homomorphic filtering technique resulted in smooth envelope enabling easy peak detection. Peak conditioning was performed to remove peaks, which do not correspond to S1 and S2. K-means clustering of the time intervals between peaks was used to indicate the occurrence of single cardiac cycles and also to point to missed cycles. Appreciable S1 and S2 amplitudes as compared to murmurs enhanced the performance of this algorithm. Feature vectors were formed after segmentation by using Daubechies-2 wavelet detail coefficients at the second decomposition level. These feature vectors were then used as input to the neural networks. Grow and Learn (GAL) and Multilayer Perceptron-Backpropagation (MLP-BP) neural networks were used for classification of three different HSs (Normal, Systolic murmur and Diastolic murmur). It was observed that the classification performance of GAL was similar to MLP-BP. However, the training and testing times of GAL were lower as compared to MLPBP. The proposed framework could be a potential solution for automatic analysis of HSs that may be implemented in real time for classification of HSs [32].

Segmentation using nonlinear dynamic analysis and high-frequency decomposition

An effective methodology for segmenting the temporal trace of PCG signals (shown in Fig. 7) is presented by Quiceno et al. [35]. Initially, inter-beat segmentation is carried out using the standard bipolar Lead-II of the ECG recording for locating the occurrence of S1. Next, the intra-beat segmentation is achieved by using Recurrence Time Statistics (RTS), which is sensitive to changes of the reconstructed attractor in a state space derived from non-linear dynamic analysis. If the segmentation using RTS fails, an alternative segmentation is proposed using thresholding over the Shannon envelogram extracted from the high-frequency decomposition. The database of PCG records, which was used, belongs to the National University of Colombia. Inter-beat segmentation accuracy was 100% over all PCG recordings. Taking into account 360 PCG beats, where a set of 180 beats were strongly

disturbed by different types of cardiac murmurs, intra-beat segmentation yielded an accuracy result of 97.7% [35].

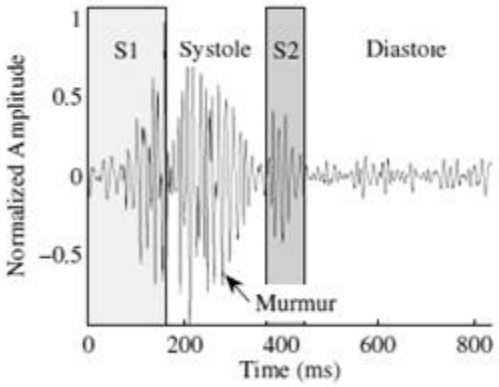

Fig. 7 Correctly segmented PCG signal with systolic murmur
(figure redrawn from Quiceno et al. [35])

Recurrence time statistics (RTS)

RTS are used in order to detect abrupt changes in the signal dynamics, corresponding to S1 and S2. An arbitrary state a_{ref} is chosen on the trajectory whereupon all recurrences within a hyper sphere of radius (r) are selected, i.e., $B_r(a_{ref}) = a$: $||a - a_{ref}|| \leq r$. Ψ is then defined as the total amount of states in the set B_r, and related to the information dimension via a power law, which motivates its ability to detect weak signal transitions based on the amplitude, period, dimension and complexity of the signal. A sliding window is used to partition the recorded PCG signal into overlapping segments, and Ψ is calculated for each segment. The r value is a very important parameter in the detection algorithm. If it is chosen too low, the hyper sphere would be low on data, and if r is chosen too high, the hyper sphere will contain misleading information from erroneous parts of the reconstructed state space. In this work, r is adaptive, and it becomes lower if there is not lobe detection corresponding to S1 and S2 in $\Psi(r)$ [34].

Wavelet decomposition and Shannon energy

These methods are used in the detection of S2 when it is considered that RTS did not give a good estimation of the boundaries. Basically, three steps are implemented: high pass filtering, wavelet decomposition and Shannon energy operator applied to the detail coefficients. From the knowledge of cardiac functionality and genesis of S1 and S2 sounds, it is known that aortic valves close with relatively large pressure difference across the valve, which originates the high frequency content in S2 sound [2]. This is the motivation to use the approximation coefficients to perform the detection of S2. To extract the signal envelope from the detail coefficients, the Shannon energy operator is applied [33].

$$E_d\left(d_j[n]\right) = -\frac{1}{N}\sum_{n=1}^{N}\left(d_j[n]\right)^2 \log\left(d_j[n]\right)^2 \tag{19}$$

where d_j are the j^{th} level detail coefficients of the wavelet transformed heart sound signal, and N is the number of samples in the selected window. This technique emphasizes the medium intensity signal components and attenuates the effect of low intensity components [34]. Using the signal envelopes provided by the Shannon energy, sound lobe boundaries are identified applying decision rules based on thresholds.

Cluster analysis and classification

Amit et al. [39] describe a computational analysis framework for identifying distinct morphologies of heart sounds and classifying them into physiological states. The analysis framework is based on hierarchical clustering, compact data representation in the feature space of cluster distances and a classification algorithm. Amit et al. [39] applied the proposed framework on two heart sound datasets, acquired during controlled alternations of the physiological conditions, and analyzed the morphological changes induced to S1, and the ability to predict physiological variables from the morphology of S1. On the first dataset of 12 subjects, acquired while modulating the respiratory pressure, the algorithm achieved an average accuracy of 82±7% in classifying the level of breathing resistance, and was able to estimate the instantaneous breathing pressure with an average error of 19±6%. A strong correlation of 0.92 was obtained between the estimated and the actual breathing efforts. On the second dataset of 11 subjects, acquired during pharmacological stress tests, the average accuracy in classifying the stress stage was 86±7%. The effects of the chosen raw signal representation, distance metrics and classification algorithm on the performance were studied on both real and simulated data. The results suggest that quantitative heart sound analysis may provide a new non-invasive technique for continuous cardiac monitoring and improved detection of mechanical dysfunctions caused by cardiovascular and cardiopulmonary diseases.

The S1 can be represented in three different forms, i.e.,

1. Time-domain representation: Direct characterization of the signal as a time series of sampled amplitude values.
2. Frequency-domain representation: Spectral characterization of the signal obtained by applying fast Fourier transforms (FFT).
3. Time-frequency representation: Joint time-frequency characterization of the signal obtained by applying one of the following transforms:

- Short-time Fourier transform (STFT), defined by:

$$S(t,f)=\int_{-\infty}^{\infty} s(\tau-t)e^{-i2\pi ft}d\tau \tag{20}$$

- S-transform (ST), defined by [43]:

$$S(t,f)=\int_{-\infty}^{\infty} s(t)\frac{|f|}{\sqrt{2\pi}}e^{-(t-\tau)^2 f^2/2}e^{-i2\pi ft}d\tau \tag{21}$$

- Wigner-Ville Distribution (WVD), defined by [44];

$$S(t,f)=\int_{-\infty}^{\infty} s\left(t+\frac{\tau}{2}\right)s^*\left(t-\frac{\tau}{2}\right)e^{-i2\pi ft}d\tau \tag{22}$$

- Choi-Williams Distribution (CWD), defined by [44];

$$S(t,f)=\int_{-\infty}^{\infty} e^{-i2\pi ft}\int_{-\infty}^{\infty}\sqrt{\frac{\sigma}{4\pi\tau^2}e^{-\sigma(\mu-t)^2/4\tau^2}}\times s\left(\mu+\frac{\tau}{2}\right)s^*\left(\mu-\frac{\tau}{2}\right)d\mu d\tau \tag{23}$$

Hierarchical clustering was applied to S1 signals, using each of the signal representations described above. The purpose of clustering is to partition a dataset into disjoint subsets (clusters), such that data elements within the same cluster share some sort of similarity. Similarity between data elements is measured using a distance metric that is suitable for the nature of the analyzed data. Two distance metrics were considered in this study:

1. Euclidean distance:

$$D_{ST} = \| s_t - r_t \|^2 = \sum_t (s_t - r_t)^2 \tag{24}$$

where s_t and r_t are signals of length n.

2. Cross-correlation:

$$D_{ST} = 1 - \frac{\sum_t (s_t - \acute{s})(r_t - \acute{r})}{\sqrt{\sum_t (s_t - \acute{s})^2} \sqrt{\sum_t (r_t - \acute{r})^2}} \tag{25}$$

where $\acute{s} = \frac{1}{n}\sum_{t-1}^{n} s_t$, $\acute{r} = \frac{1}{n}\sum_{t-1}^{n} r_t$.

Clustering was done using an agglomerative hierarchical clustering procedure that initially partitions a set of n data elements into n clusters, each containing one data element, and then iteratively merges the two most similar clusters, until the entire dataset forms a single cluster [45]. The bottom of the created hierarchical tree can next be pruned so that the required number of clusters N is obtained. Each cut of the data elements are assigned to a single cluster, creating the output data partitioning to clusters $\{C_1, \ldots, C_N\}$. The algorithm requires a cluster similarity criterion for choosing the next two clusters to be merged. Authors in [46] have used Ward's step-wise optimal criterion, which chooses the clusters such that the increase in the overall sum-of-squared error after the merge is minimal. The distance between clusters C_i and C_j is defined by: $D_w(C_i, C_j) = \sqrt{n_i n_j} / n_i + n_j \| m_i - m_j \|$, where n_i, and n_j are the sizes of clusters, and m_i, and m_j are their means.

LMS based least square SVM classifier

Here, a technique to improve the performance of the Least Square Support Vector Machine (LSSVM) is proposed for classification of normal and abnormal heart sounds using wavelet based feature set. In the proposed technique, the Lagrange multiplier is modified based on Least Mean Square (LMS) algorithm, which in turn modifies the weight vector to reduce the classification error. The basic idea is to enlarge the separating boundary surface, such that the separability between the clusters is increased. The updated weight vector is used at the time of testing. The performance of the proposed systems is evaluated on 64 different recordings of heart sounds comprising of normal and five different pathological cases. It is found that the proposed technique classifies the heart sounds with higher recognition accuracy than competing techniques [59].

Hilbert transfer

The key features of PCG are extracted based on the slopes of envelop of Hilbert Transfer after relocating boundaries with energy envelope segmentation [69].

$$H\left(x(t)\right)=\frac{1}{\pi}\int_{-\infty}^{+\infty}\frac{x(\tau)}{t-\tau}d\tau \tag{26}$$

$$Z(x)=x(t)+H\left(x(t)\right) \tag{27}$$

where $H(x(t))$ is the Hilbert transferred signal. The mode of $Z(x)$ is the original envelope.

The overall accuracy of features extraction is found to be 91.95%. 25 significant clinical features are introduced, and chosen to make two-kind classification by SVM. In the results of two-kind classification, the overall accuracy is 91.3%, which is better than 85.23% accuracy in 100 features of Shannon Energy Envelope. The result shows that features including clinical signification is of signification for enhancing the accurate rate of PCG classification [70].

Wavelet packet entropy

Wavelet transform is a powerful technique in analyzing nonstationary signals such as PCG signals [77]. The main advantage of wavelet transform is its varying window size that is narrow for high frequencies and wide for low frequencies. Therefore, wavelet transform is much more powerful than the other time frequency analysis techniques such as Discrete Fourier Transform (DFT) and Short-Term Fourier Transform (STFT), not only for providing useful time and frequency information, but also for its adaptive time and frequency resolution [78].

A. Wavelet packet transform (WPT)

WPT is an extension of Discrete Wavelet Transform (DWT) whereby all nodes in the tree structure are allowed to split further at each level of decomposition. With WPT, both the approximation and detail coefficients are decomposed into approximation and detail components. In comparison to DWT, WPT decomposes only the approximation coefficients of the signal (as shown in Fig. 8). Therefore, features can be generated based on approximation and detail coefficients at different levels to obtain more information. The WPT of a signal $x(t)$ is defined as follows:

$$x_p^{n,j}=2^{j/2}\int_R x(t)\psi_n\left(2^{-j}t-p\right)dt,\quad 0\le n\le 2^s-1 \tag{28}$$

where n is the channel number, j is the number of decomposition level, or scale parameter, p is the position parameter, $\psi_n(t)$ is the mother wavelet, and S is the maximum decomposition level. After decomposing signal $x(t)$ by WPT, 2^S sequences can be produced in the S^{th} level. The fast decomposition equation for this kind of WPT is

$$x_k^{2n,j+1}=\sum_{p\in Z}h(p-2k)x_p^{n,j}$$

$$x_k^{2n+1,j+1}=\sum_{p\in Z}g(p-2k)x_p^{n,j} \tag{29}$$

where $h(i)$ and $g(i)$ are wavelet quadrature mirror filter coefficients.

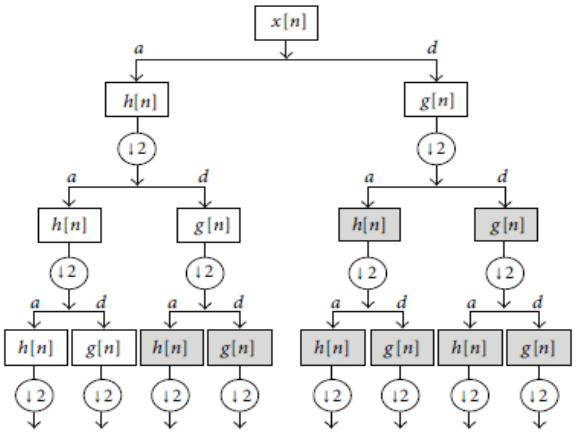

Fig. 8 Wavelet packet tree with corresponding high-pass and low-pass filters (a = approximation coefficients, d = detail coefficients).
The shaded nodes indicate the node not to be produced by DWT.

Three levels of the wavelet packet decomposition with the high-pass and low-pass filters were illustrated in Fig. 8. This structure can be continued further to decompose the following approximations and details to reach to a proper level for representing PCG signals of desired murmurs. From the literature, it can be concluded that levels 6 to 8 were generally chosen for analyzing PCG signals of different pathological heart sounds [79-83].

B. Entropy

Different types of entropy such as log, norm, Shannon, sure, and threshold can be used to characterize the heart sounds. However, for this study the entropy introduced by Vitulano and Casanova [84] for analyzing 1D signals was utilized. They have transformed the 2D mammographic signal into 1D signal through linear transformation and then applied the entropy on the 1D signal to generate features for differentiating mammograms with different pathologies. They did not utilize any signal processing technique to analyze the signal prior to extract entropy features from the signal. In the current study, the PCG signals were first analyzed with WPT and then entropy features were generated from the wavelet packet coefficients. Vitulano and Casanova [84] defined the signal "crest" as the part embraced between lines parallel to the abscissas axis, in which the ordinates are m and M, m is the absolute minimum and M is the absolute maximum of the signal. Therefore, the signal crest included all the points $x(t) \in X(t)$, so that

$$m \le x(t) \le M \tag{30}$$

and crest energy is defined as

$$E_c = \sum_{i=m}^{M} x_i,\ i \equiv [m, M] \tag{31}$$

Signal entropy can be defined based on E_c as

$$S = 1 - \frac{E - E_c}{E},\ S \equiv [0, 1] \tag{32}$$

where E is signal energy, E_c is crest energy, and S is signal entropy. Signal entropy S is defined based on one-dimensional signals and it has a potential to be applied on the other dimensional signals such as PCG signals.

Safara et al. [85] employed wavelet packet transform for heart sound analysis, and the entropy was calculated for deriving feature vectors. Five types of classification were performed to evaluate the discriminatory power of the generated features. The best results were achieved by BayesNet with 96.94% accuracy.

Conclusion

The PCG signal confirms, and mostly, refines the auscultation data and provides further information about the acoustic activity concerning the chronology of the pathological signs in the cardiac cycle, by locating them with respect to the normal heart sounds. Heart murmurs are the first signs of cardiac valve disorders. Several studies have been conducted in recent years to automatically differentiate normal heart sounds from heart sounds with murmurs using various types of audio features. The heart sound categories would be expanded to include different murmurs. Few methods are discussed for feasible way to enhance the accurate rate of Phonocardiogram classification. This review also suggests quantitative heart sound analysis may provide a new non-invasive technique for continuous cardiac monitoring and improved detection of mechanical dysfunctions caused by cardiovascular and cardiopulmonary diseases. The first part of this review represents the significance of PCG signal and the second part demonstrates the different methodology involved for detection, classification and analysis of PCG signal.

References

1. Goldberger A. L. (1992). Fractal Mechanisms in the Electrophysiology of the Heart, IEEE Eng Med Biol Mag, 26, 47-52.
2. Leatham A. (1975). Auscultation of the Heart and Phonocardiography, Churchill Livingstone, New York.
3. Vepa J. (2009). Classification of Heart Murmurs Using Cepstral Features and Support Vector Machines, In Engineering in Medicine and Biology Society, Annual International Conference of the IEEE, 2539-2542.
4. Zhang Y-T., G. Chan, X-Y. Zhang, L. Yip (2006). Heart Sounds and Stethoscopes, In: Wiley Encyclopedia of Biomedical Engineering, Akay M. (Ed.), Wiley-Interscience, Wiley and Sons, Hoboken, N.J., 1824-1834.
5. Tilkian A. G., M. B. Conover (2001). Understanding Heart Sounds and Murmurs: with an Introduction to Lung Sounds, Saunders, Philadelphia, 4th Edition.
6. Kingsley B. (1972). Acoustic Evaluation of Prosthetic Cardiac Valve in the Audio Spectrum, Journal of Audio Engineering Society, 20(9), 750-755.
7. Geckeler G. D., W. Likoff, D. Mason, R. R. Riesz, C. H. Wirth (1954). Cardiospectrograms: A Preliminary Report, Amer Heart J, 48, 189-196.
8. McKusic V. A., S. A. Talbot, G. N. Weeb (1954). Spectral Phonocardiography: Problems and Prospects in the Application of the Bell Sound Spectrograph to Phonocardiography, Bull Johns Hopkins Hosp, 94, 187-198.
9. Hylen J. C., F. E. Kloster, R. H. Herr, A. Starr, H. E. Griswold (1969). Sound Spectrographic Diagnosis of Ball Variance, Circulation, XXXIX, 849-858.
10. Aigner V. A., G. Muller, E. Knapp, E. Raas (1973). Schallspektrographische Untersuchungen an Starr-Edwards-Aortenkl appenprotesen, Z Cardiol, 62, 1105-1113. (in German)

11. Aigner V. A. (1977). Kontursonagraphische Analysen von Herzschall-Phgnomenen und Tbnen verschiedener Klappenprothesen Fortschr, Med, 95, 2162-2166. (in German)
12. Kagawa Y., S. Nitta, S. Naoshi, S. Komei, Y. Shibota, T. Horiuchi, T. Motonao (1977). Sound Spectroanalytic Diagnosis of Malfunctioning Prosthetic Heart Valve, Tohoku J Exp Med, 123, 77-89.
13. Cooley J. W., J. W. Tukey (1965). An Algorithm for Machine Calculation of Complex Fourier Series, Math Computation, 19, 297-301.
14. Rabiner L. R., R. W Schafer (1978). Digital Processing of Speech Signals, Chapter 6, Prentice-Hall, Englewood Cliffs, N.J., 250-354.
15. Durand L.-G., J. de Guise, R. Guardo (1980). FFT Techniques for the Spectral Analysis of Prosthetic Heart Valve Sounds, Proc Annu Symp Comput Appl Med Care, 2, 1105-1111.
16. Nagel J. (1986). New Diagnostic and Technical Aspects of Fetal Phonocardiography, European Journal of Obstetrics & Gynecology and Reproductive Biology, 23(5-6), 295-303.
17. Mallat S. G., Z. Zhang (1993). Matching Pursuits with Time-frequency Dictionaries, IEEE Trans Signal Processing, 41, 3397-3415.
18. Zhang X., L.-G. Durand, L. Senhadji, H. C. Lee, J.-L. Coatrieux (1998). Time-frequency Scaling Transformation of the Phonocardiogram Based of the Matching Pursuit Method, IEEE Transactions on Biomedical Engineering, 45(8), 972-979.
19. Owsley N. L. (2000). Array Phonocardiography, The IEEE 2000 Adaptive Systems for Signal Processing, Communications, and Control Symposium, AS-SPCC, 31-36.
20. Austin A., A. Hull, N. Owsley, M. Peloquin (1997). Device and Method for Locating Flow Blockage in a Three-dimensional Object, United States Patent 5,617,869, Filed: 16 June 1995, Issued: 8.
21. Owsley N. L. (1998). Method and Apparatus for Noninvasive Detection and Analysis of Turbulent Flow in a Patient's Blood Vessels, United States Patent 5,727,561, Filed: 23 April 1996, Issued: I7.
22. Qwsley N. L., A. Hull (1998). Beam Formed Near Field Imaging of a Simulated Coronary Artery Containing a Stenosis, IEEE Trans on Medical Imaging, 37(6), 900-909.
23. Rice M. L., D. J. Doyle (1995). Comparison of Phonocardiographic Monitoring Location, IEEE 17th Annual Conference Engineering in Medicine and Biology Society, 1, 685-686.
24. Hansen P. B., A. A. Luisada, D. J. Miletich (1989). Phonocardiography as a Monitor of Cardiac Performance during Anesthesia, Anesth Anulg, 68, 385-387.
25. Durand L. G., Y. E. Langlois, T. Lanthier (1990). Spectral Analysis and Acoustic Transmission of Mitral and Aortic Valve Closure Sounds in Dogs, Part 4: Effects of Modulating Cardiac Inotropy, Med Biol Eng Comput, 28, 439-445.
26. Luisada A. A., A. Singhal, F. Portaluppi, C. Strozzi (1985). Noninvasive Index of Cardiac Contractility during Stress Testing: A Collaborative Study, Clin Cardiol, 8(7), 375-384.
27. Luisada A. A., A. Singhal, V. Knigten (1986). New Index of Cardiac Contractility during Stress Testing with Treadmill, Acta Curdiol, 41(1), 31-39.
28. Luisada A. A., A. Singhal, F. Portaluppi (1985). Assessment of Left Ventricular Function by Noninvasive Methods, Adv Curdiol, 32, 111-141.
29. Xiao S., Sh. Cai, G. Liu (2000). Studying the Significance of Cardiac Contractility Variability Analyzing the Influence of Respiration, Exercise, and Psychological Activity Using Heart-sound Analysis, IEEE Engineering in Medicine and Biology Magazine, 19(3), 102-105.
30. Jain A. K., A. Ross, S. Prabhakar (2004). An Introduction to Biometric Recognition, IEEE Trans Circuits Syst Video Technol, Special Issue Image- and Video-based Biomet, 14(1), 4-20.

31. Beritelli F., S. Serrano (2007). Biometric Identification Based on Frequency Analysis of Cardiac Sounds, IEEE Transactions on Information Forensics and Security, 2(3), 596-604.
32. Gupta C. N., R. Palaniappan, S. Swaminathan, S. M. Krishnan (2007). Neural Network Classification of Homomorphic Segmented Heart Sounds, Applied Soft Computing, 7, 286-297.
33. El-Segaier M., O. Lilja, S. Lukkarinen, L. Srnmo, R. Sepponen, E. Pesonen (2005). Computer-based Detection and Analysis of Heart Sound and Murmur, Ann Biomed Eng, 33(7), 937-942.
34. Ahlstrom C., O. Liljefeldt, P. Hult, P. Ask (2005). Heart Sound Cancellation from Lung Sound Recordings Using Recurrence Time Statistics and Nonlinear Prediction, IEEE Signal Processing Letters, 12(12), 812-815.
35. Quiceno A. F., E. Delgado, M. Vallverd, A. M. Matijasevic, G. Castellanos-Domnguez (2008). Effective Phonocardiogram Segmentation Using Nonlinear Dynamic Analysis and High-frequency Decomposition, Computers in Cardiology, 35, 161-164.
36. Tavel M. E. (1978). Clinical Phonocardiography & External Pulse Recording, Third ed., Year Book Medical Publishers Inc., Chicago.
37. Sakamoto T. (1965). Hemodynamic Determinants of the Amplitude of the First Heart Sound, Circ Res, 16, 45-57.
38. Clarke W. B., S. M. Austin, M. S. Pravib, P. M. Griffen, J. T. Dove, J. McCullough, B. F. Schreiner (1978). Spectral Energy of the First Heart Sound in Acute Myocardial Ischemia, Circulation, 57, 593-598.
39. Amit G., N. Gavriely, N. Intrator (2009). Cluster Analysis and Classification of Heart Sounds, Biomedical Signal Processing and Control, 4, 26-36.
40. Durand L. G., M. Blanchard, G. Cloutier, H. N. Sabbah (1990). Comparison of Pattern Recognition Methods for Computer Assisted Classification of Spectra of Heart Sounds in Patients with a Porcine Bioprosthetic Valve Implanted in the Mitral Position, IEEE Trans Biomed Eng, 37(12), 1121-1129.
41. Guo Z., L. G. Durand, H. C. Lee, L. Allard, M. C. Grenier, P. D. Stein (1994). Artificial Neural Networks in Computer-assisted Classification of Heart Sounds in Patients with Porcine Bioprosthetic Valves, Med Biol Eng Comput, 32(3), 311-316.
42. Bentley P. M., P. M. Grant, J. T. McDonnell (1998). Time-frequency and Time-scale Techniques for the Classification of Native and Bioprosthetic Heart Valve Sounds, IEEE Trans Biomed Eng, 45(1), 125-128.
43. Stockwell R. G., L. Mansinha, R. P. Lowe (1996). Localization of the Complex Spectrum: The S-transform, IEEE Trans Signal Process, 44(4), 998-1001.
44. Cohen L. (1989). Time-frequency Distributions – A review, Proceedings of the IEEE, 77(7), 941-981.
45. Johnson S. C. (1967). Hierarchical Clustering Schemes, Psychometrika, 2, 241-254.
46. Ward J. H. (1963). Hierarchical Grouping to Optimize an Objective Function, J Am Stat Assoc, 58(301), 236-244.
47. Hanna I. R., M. E. Silverman (2002). A History of Cardiac Auscultation and Some of its Contributors, The American Journal of Cardiology, 90, 259-267.
48. Bender J. R. (1992). Yale University School of Medicine Heart Book, New York: William Morrow and Company, Inc., 167-175.
49. Tavel M. E. (1996). Cardiac Auscultation: A Glorious Past-but does it Have a Future? Circulation, 93, 1250-1253.
50. Shub C. (2003). Echocardiography or Auscultation? How to Evaluate Systolic Murmurs? Canadian Family Physician, 49, 163-167.

51. Chizner M. A. (2008). Cardiac Auscultation: Rediscovering the Lost Art, Current Problems in Cardiology, 33, 326-408.
52. Cromwell L., F. J. Weibell, E. A. Pfeiffer (2002). Biomedical Instrumentation and Measurements, 2nd Ed., PHI Publication, 169-172.
53. Rangayyan R. M. (2002). Biomedical Signal Analysis, IEEE Press, John Wiley & Sons Inc, 34-38.
54. Cathers I. (1995). Neural Network Assisted Cardiac Auscultation, Artificial Intelligence in Medicine, 7, 53-66.
55. Ölmez T., Z. Dokur (2003). Classification of Heart Sounds Using an Artificial Neural Network, Pattern Recognition Letters, 24, 617-629.
56. Reed T. R., N. E. Reed, P. Fritzson (2004). Heart Sound Analysis for Symptom Detection and Computer-aided Diagnosis, Simulation Modeling Practice and Theory, 12, 129-146.
57. Ari S., G. Saha (2007). On a Robust Algorithm for Heart Sound Segmentation, Journal of Mechanics in Medicine and Biology, 7(2), 129-150.
58. Choi S. (2008). Detection of Valvular Heart Disorders Using Wavelet Packet Decomposition and Support Vector Machine, Expert Systems with Application, 35, 1679-1687.
59. Ari S., K. Hembram, G. Saha (2010) Detection of Cardiac Abnormality from PCG Signal Using LMS Based Least Square SVM Classifier, Expert Systems with Applications, 37, 8019-8026.
60. Xu J., L. Durand, P. Pibarot (2000). Nonlinear Transient Chirp Signal Modeling of the Aortic and Pulmonary Components of the Second Heart Sound, IEEE Trans Biomed Eng, 47(7), 1328-1335.
61. Xu J., L. Durand, P. Pibarot (2001). Extraction of the Aortic and Pulmonary Components of the Second Heart Sound Using a Nonlinear Transient Chirp Signal Model, IEEE Trans Biomed Eng, 48(3), 277-283.
62. Baykal A., Y. Z. Ider, H. Koymen (1995) Distribution of Aortic Mechanical Prosthetic Valve Closure Sound Model Parameters on the Surface of the Chest, IEEE Trans Biomed Eng, 42(4), 358-370.
63. Koymen H., B. K. Altay, Y. Z. Ider (1987). A Study of Prosthetic Heart Valve Sounds, IEEE Trans Biomed Eng, 34(11), 853-863.
64. Sava H. P., J. T. E. McDonnell (1995). Modified Forward-backward Over Determined Prony's Method and its Application in Modeling Heart Sounds, IEEE Proceedings – Vision, Image and Signal Processing, 142(6), 375-380.
65. Leung T. S., P. R. White, W. B. Cook (1998). Analysis of the Second Heart Sound for Diagnosis of Paediatric Heart Disease, IEEE Proc. – Sci Meas Technol, 145(6), 285-290.
66. Maneejiraprakarn N., P. Panpho, D. Boonthong, P. Thitiwuthikiat, J. Koseeyaporn, P. Wardkein (2006). Low Cost Non-invasive Instrument for Heart Disease and Peripheral Vascular Disease Detection, Biomedical Circuits and Systems Conference, IEEE Biomedical Circuits and Systems Conference, 49-52.
67. Debbal S. M., F. Bereksi-Reguig (2008). Computerized Heart Sounds Analysis, Computers in Biology and Medicine, 38, 263-280.
68. Debbal S. M., F. Bereksi-Reguig (2007). Automatic Measure of the Split in the Second Cardiac Sound by Using the Wavelet Transform Technique, Computers in Biology and Medicine, 37, 269-276.
69. Tu Z., G. Cao, Q. Li, X. Zhang, J. Shi (2010). Improved Methods for Detecting Main Components of Heart Sounds, Sixth International Conference on Natural Computation, 7, 3585-3588.

70. Hu X.-J., G.-T. Cao, H.-H. Zhu, H. Li (2011). Feature Extraction and Choice in PCG Based on Hilbert Transfer, 4th International Congress on Image and Signal Processing, IEEE, 4, 2159-2163.
71. Rangayyan R. M., R. J. Lehner (1988). Phonocardiogram Signal Analysis: A Review, CRC Critical Reviews in Biomedical Engineering, 15(3), 211-236.
72. Durand L. G., M. Blanchard, G. Cloutier, H. N. Sabbah, P. D. Stein (1990). Comparison of Pattern Recognition Methods for Computer-assisted Classification of Spectra of Heart Sounds in Patients with a Porcine Bioprosthetic Valve Implanted in the Mitral Position, IEEE Trans Biomed Eng, 37(12), 1121-1129.
73. Durand L. G., M. Blanchard, H. N. Sabbah, P. D. Stein (1991). Comparison of Spectral Techniques for Computer Assisted Classification of Spectra of Heart Sounds in Patients with a Porcine Bioprosthetic Valves, Med Biol Eng Comput, 31(3), 229-236.
74. Durand L. G., P. Pibarot (1995). Digital Signal Processing of the Honocardiogram: Review of the Most Recent Advancements, Critical Reviews in Biomedical Engineering, 23(3/4), 163-219.
75. Sarbandi R. R., D. D. Doyle, M. Navidbakhsh, K. Hassani, H. Torabiyan (2011). Color Spectrographic Phonocardiography (CSP) Applied to the Detection and Characterization of Heart Murmurs: Preliminary Results, BioMedical Engineering OnLine, 10:42, doi: 10.1186/1475-925X-10-42.
76. Akbari M. A., K. Hassani, J. D. Doyle, M. Navidbakhsh, M. Sangargir, K. Bajelani, Z. S. Ahmadi (2011). Digital Subtraction Phonocardiography (DSP) Applied to the Detection and Characterization of Heart Murmurs, BioMedical Engineering OnLine, 10:109, doi: 10.1186/1475-925X-10-109.
77. Ergen B., Y. Tatar, H. O. Gulcur (2011). Time-frequency Analysis of Phonocardiogram Signals Using Wavelet Transform: A Comparative Study, Computer Methods in Biomechanics and Biomedical Engineering, 15, 371-381.
78. Chen Y., S. Wang, C.-H. Shen, F. K. Choy (2012). Matrix Decomposition Based Feature Extraction for Murmur Classification, Medical Engineering & Physics, 34(6), 756-761.
79. Choi S., Y. Shin, H. K. Park (2011). Selection of Wavelet Packet Measures for Insufficiency Murmur Identification, Expert Systems with Applications, 38(4), 4264-4271.
80. Ahlstrom C., P. Hult, P. Rask (2006). Feature Extraction for Systolic Heart Murmur Classification, Annals of Biomedical Engineering, 34(11), 1666-1677.
81. Choi S. (2008). Detection of Valvular Heart Disorders Using Wavelet Packet Decomposition and Support Vector Machine, Expert Systems with Applications, 35(4), 1679-1687.
82. Debbal S. M., F. Bereksi-Reguig (2007). Time-frequency Analysis of the First and the Second Heartbeat Sounds, Applied Mathematics and Computation, 184(2), 1041-1052.
83. Homaeinezhad M. R., S. A. Atyabi, E. Deneshvar, A. Ghaffari, M. Tahmasebi (2011). Optimal Delineation of PCG Sounds via False-alarm Bounded Segmentation of a Wavelet-based Principal Components Analyzed Metric, International Journal for Numerical Methods in Biomedical Engineering, 27, 1711-1739.
84. Vitulano S., A. Casanova (2008). The Role of Entropy: Mammogram Analysis, Image Analysis and Recognition, 5112, 863-872.
85. Safara F., S. Doraisamy, A. Azman, A. Jantan, S. Ranga (2012). Wavelet Packet Entropy for Heart Murmurs Classification, Advances in Bioinformatics, Volume 2012, Article ID 327269.
86. Moukadem A., A. Dieterlen, C. Brandt (2012). Phonocardiogram Signal Processing Module for Auto-diagnosis and Telemedicine Applications, eHealth and Remote Monitoring, El Hassani A. H. (Ed.), InTech, doi: 10.5772/48447.

87. Sa-Ngasoongsong A., J. Kunthong, V. Sarangan, X. Cai, S. T. S. Bukkapatnam (2012). A Low-cost, Portable, High-throughput Wireless Sensor System for Phonocardiography Applications Sensors, 12, 10851-10870, doi: 10.3390/s120810851.
88. Hult P., T. Fjällbrant, B. Wranne, P. Ask (2004). Detection of the Third Heart Sound Using a Tailored Wavelet Approach, Med Biol Eng Comput, 42(2), 253-258.
89. Wiggers C. J. (1919). Factors Determining the Relative Intensity of the Heart Sounds in Different Auscultation Areasan Experimental Study, Arch Intern Med, 24(5), 471-488.
90. Dock W. (1933). Mode of Production of the First Heart Sound, Arch Intern Med, 51(5), 737-746.
91. Dean A. L (1916). The Movements of the Mitral Cusps in Relation to the Cardiac Cycle, Amer J Physiol, 40, 206-217.
92. Wolfenh C. C., A. Margolies (1945). Heart Sounds, In: Diagnosis and Treatment of Cardiovascular Disease, Stroud W. D. (Ed.), 3rd Ed., Philadelphia, F. A. Davis.

Assist. Prof. Akash Kumar Bhoi, M.Tech
E-mail: akash730@gmail.com

Akash Kumar Bhoi has completed his B.Tech. (Biomedical Engineering) from the TAT, Bhubaneswar and M.Tech. (Biomedical Instrumentation) from Karunya University, Coimbatore in the year 2009 and 2011 respectively. He is pursuing Ph.D. from Sikkim Manipal University, India. He is working as an Assistant Professor in the Department of Applied Electronics and Instrumentation at Sikkim Manipal Institute of Technology (SMIT), India since 2012. He is a member of ISEIS and IAENG, an Associate member of UACEE and Editorial Board member of IJAEEE, IJAEEE, ITSI-TEEE, IJECCE and IJCTT and a reviewer of IJET, IJCT, IJBSE, IJMI, AJBLS. His areas of research are biomedical signal processing, medical image processing, sensor and transducer and medical instrumentation. He has published papers in national and international journals and conferences. He has also published 3 book chapters. He has participated in workshops, seminars and conferences.

Prof. Karma Sonam Sherpa, Ph.D.
E-mail: karmasherpa23@gmail.com

Karma Sonam Sherpa has completed his B.E. (Electrical Engineering) from the MREC, Jaipur, and M.Tech. (Power Electronics and Machine Drives) from IIT, Kharagpur in the year 1996 and 2003 respectively. He has a Ph.D. from Sikkim Manipal University. He has been serving SMIT, Sikkim for the last sixteen years. Presently, he is a Professor in the Department of Electrical and Electronics Engineering and officiating head of the Department of Electrical and Electronics Engineering and Department of Applied Electronics and Instrumentation Engineering. He is a life member of ISTE, IEI and System Society of India. His areas of interests are electric power distribution system, power electronics and electrical drives. He has published papers in national and international journals and conferences. He has organized workshops, seminars and conferences.

Prof. Dr. Bidita Khandelwal, MD.
E-mail: drbidita@gmail.com

Dr. Bidita Khandelwal did her MD Medicine in 1998 from Assam University. She joined Sikkim Manipal Institute of Medical Sciences in 2000 as an Assistant Professor in Department of Medicine and since 2009 heads the Department. Since 2015 Dr. Bidita Khandelwal is a Professor. She is a life member of API, IMA, IACM and RSSDI. Other posts held are Chairperson of complaint committee on Sexual Harassment at work place, Chairperson of IEC, Ayurveda Regional Research Institute, Vice chairman API East Zone, Editorial Board member of IJEM, a Member of Academic Senate of SMU, a Member of Sikkim Medical Council, Coordinator post graduate studies and an External expert for Board of Study. She is a Member of Research Protocol Evaluation Committee, Publication Evaluation committee, Institutional Ethics Committee, Hospital Management Committee, Infection Control Committee, Promotion Committee, State Task Force, Pharmacovigilance Committee. She has special interest in diabetes mellitus and has several publications related to it.